Supplementary Information

Adaptive responses of *Bacillus subtilis* underlie differential nanoplastic toxicity with implications for root colonization

Franklin Perez,[1] Nesha May O. Andoy,[1] Uyen Tran Thao Hua,[1] Keiko Yoshioka,[2,3] and Ruby May A. Sullan[1,4]*

[1]Department of Physical and Environmental Sciences, University of Toronto Scarborough, 1065 Military Trail, Toronto, ON, Canada, M1C 1A4; [2]Department of Cell and Systems Biology, University of Toronto, 25 Wilcocks St., Toronto, ON, Canada, M5S 3B2; [3]Center for the Analysis of Genome Evolution and Function (CAGEF), University of Toronto, 25 Wilcocks St., Toronto, ON, Canada, M5S 3B2; [4]Department of Chemistry, University of Toronto, 80 St. George St., Toronto, ON, Canada, M5S3H6;

*email: ruby.sullan@utoronto.ca

Supplementary Figures

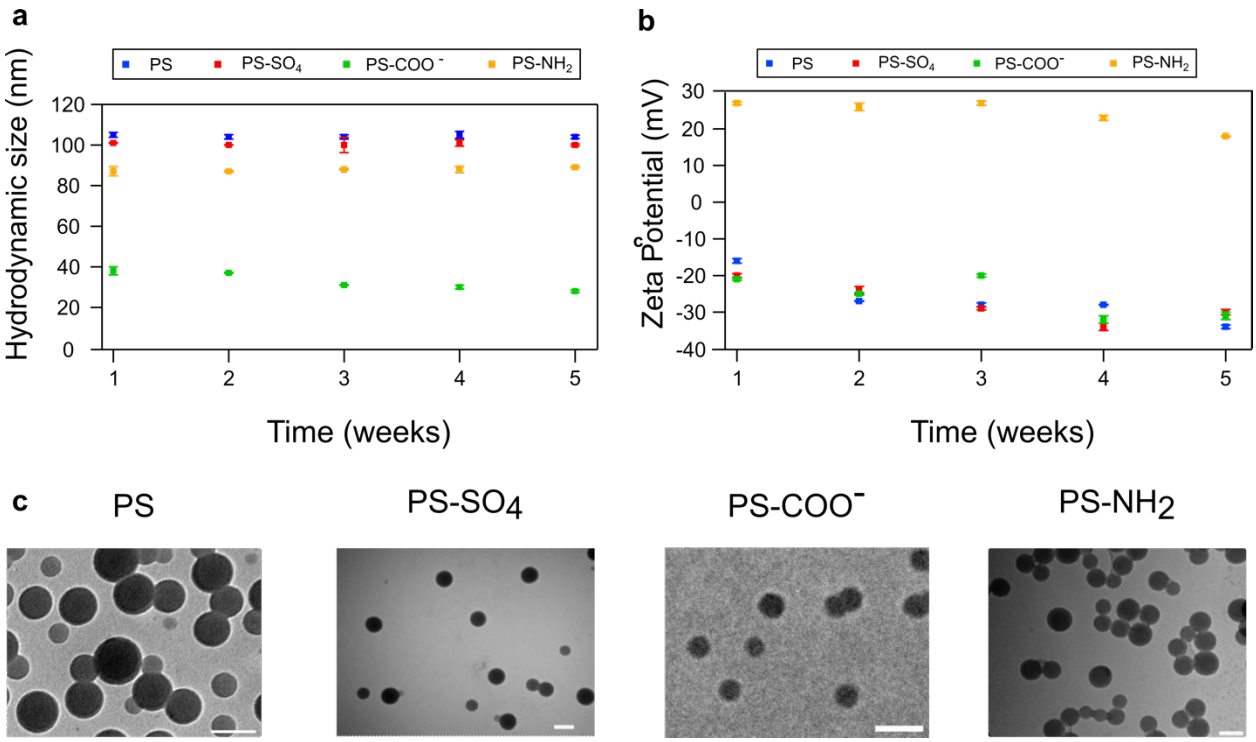

Figure S1. Nanoplastic characterization. (a) Hydrodynamic diameters obtained from Dynamic Light Scattering (DLS), (b) surface zeta potential from Phase-Analysis Light Scattering (PALS), and (c) transmission electron microscopy (TEM) images of the different model nanoplastics used in this study: 100-nm bare polystyrene (PS), 100-nm sulfate-modified polystyrene ($PS\text{-}SO_4$), 30-nm carboxylate-modified polystyrene ($PS\text{-}COO^-$), and amine-modified polystyrene nanoparticles ($PS\text{-}NH_2$). Markers in a and b represent averages of three replicates and bars are standard deviation. Scalebar in C is 100 nm.

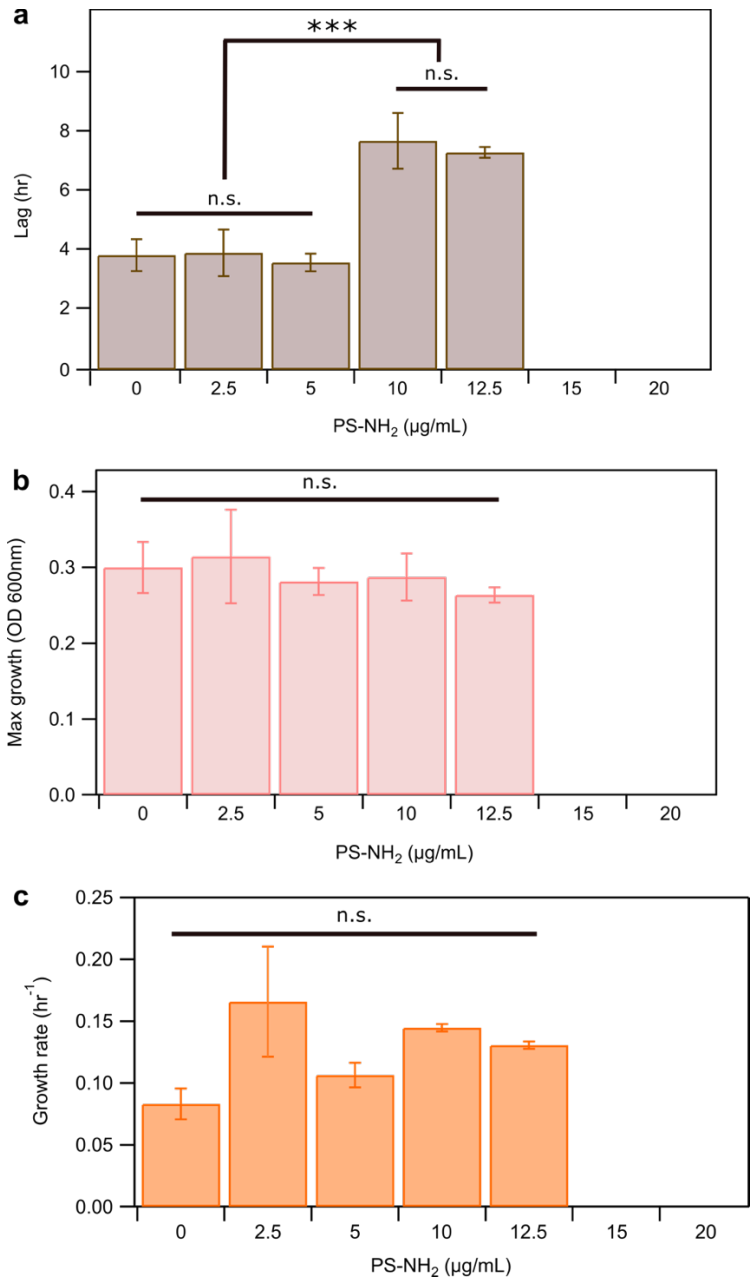

Figure S2. Analysis of bacterial growth parameters following exposure to PS-NH_2, based on the Gompertz fit of growth curves in Figure 1a. (a) Lag phase, (b) maximum (max) growth, and (c) growth rate are presented. Error bars indicate the standard deviation from at least three independent replicates. No values are shown at 15 and 20 µg/mL PS-NH_2 because no growth was observed at these concentrations. Statistical significance was assessed using One-way ANOVA, with *** denoting $p < 0.001$ and n.s. indicating non-significance.

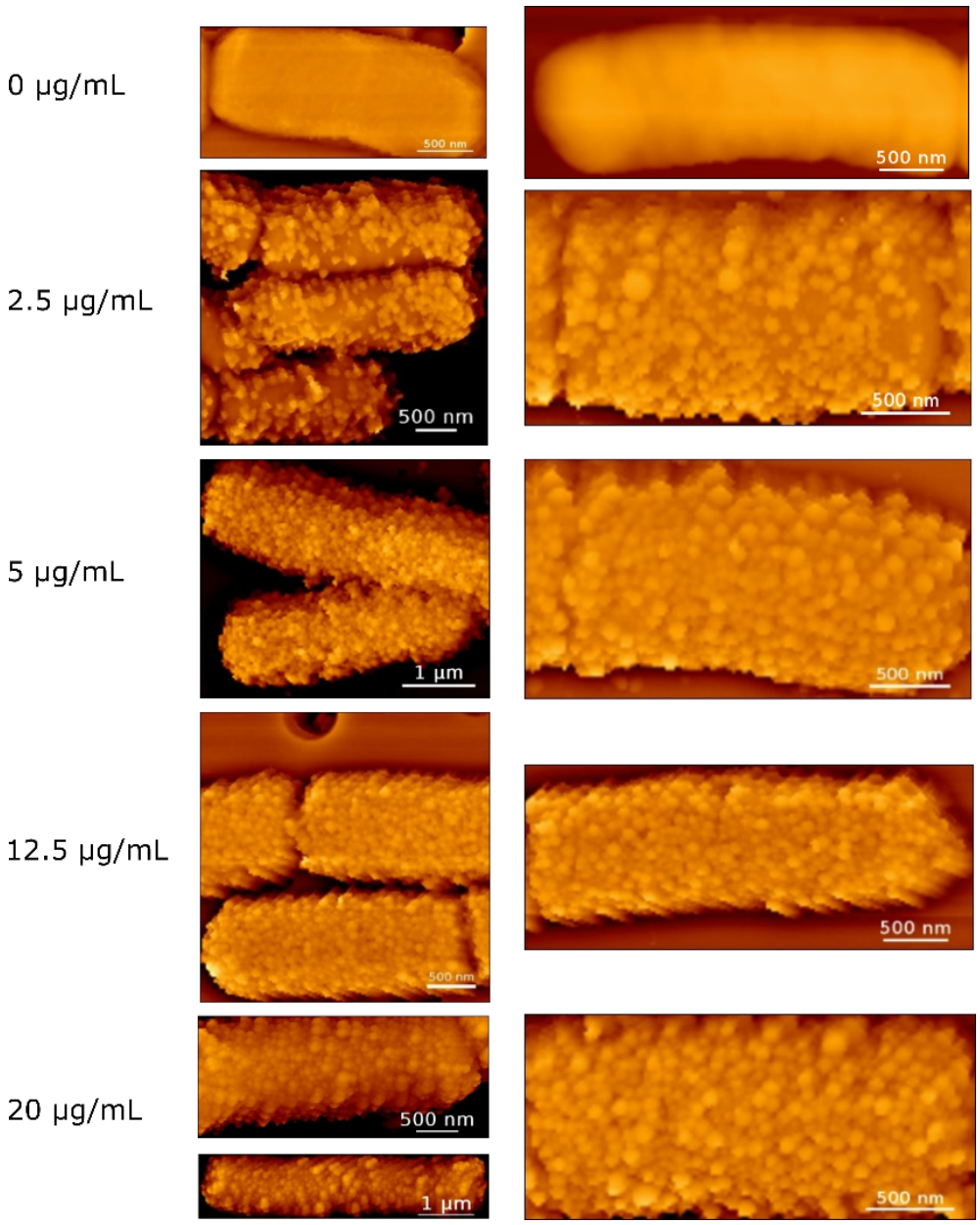

Figure S3. PS-NH_2 forms a concentration-dependent multilayer nanoplastic coating around *B. subtilis*. Atomic force microscopy (AFM) images of *Bacillus subtilis* showing concentration-dependent multilayer surface coverage of positively charged, amine-modified polystyrene nanoparticles (PS-NH_2) immediately after 30-min treatment in MilliQ water.

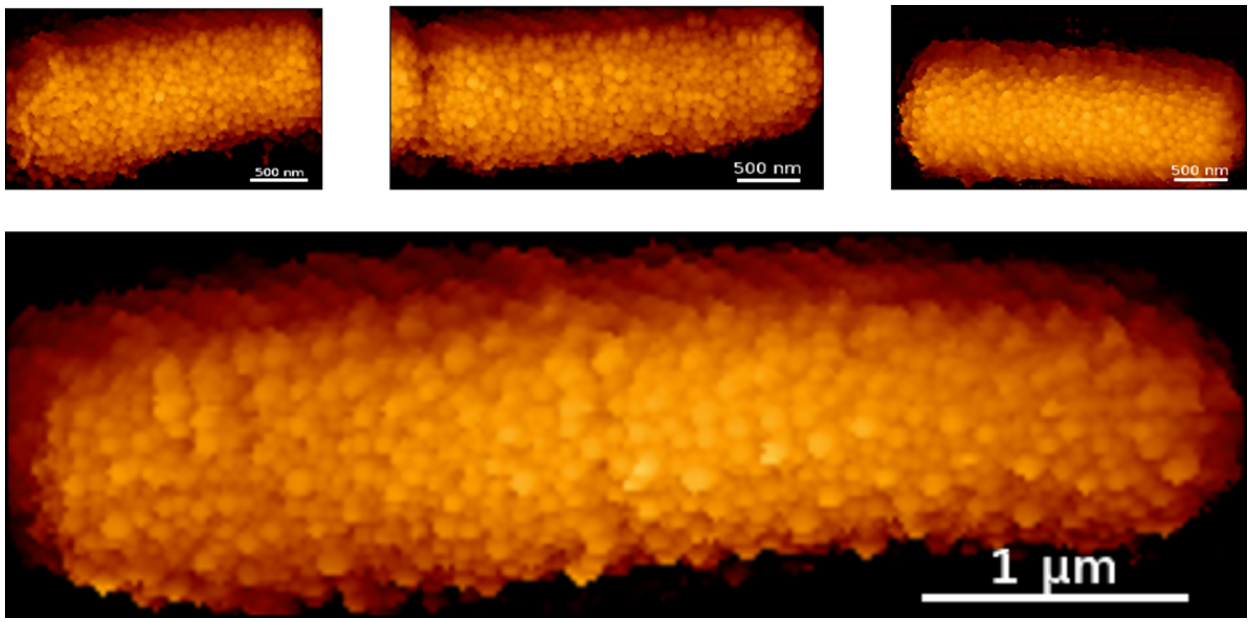

Figure S4. Bound PS-NH_2 remains firmly attached to the surface of *B. subtilis*. AFM images of PS-NH_2-teated *B. subtilis* showing the multilayer nanoplastic coating even after 12 hours of equilibration in MilliQ water (where no growth is expected to occur).

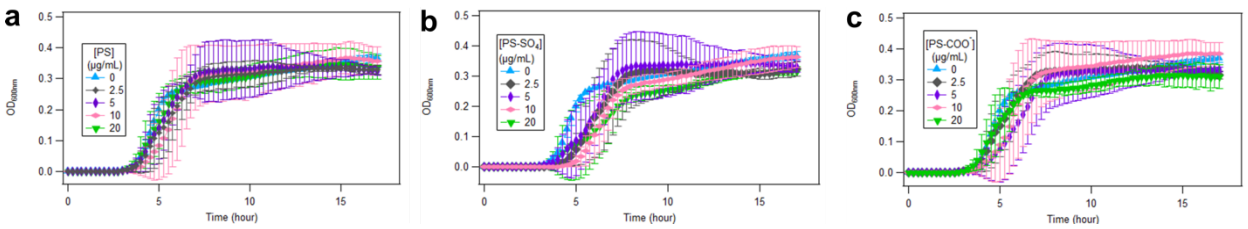

Figure S5. Negatively charged model nanoplastics did not inhibit bacterial growth. Growth curves of negatively charged nanoplastics: (a) 100-nm bare polystyrene (PS), (b) 100-nm sulfate-modified polystyrene (PS-SO_4), and (c) 30-nm carboxylate-modified polystyrene (PS-COO^-). Bars represent standard deviation of at least three replicates and data are representative of at least three trials.

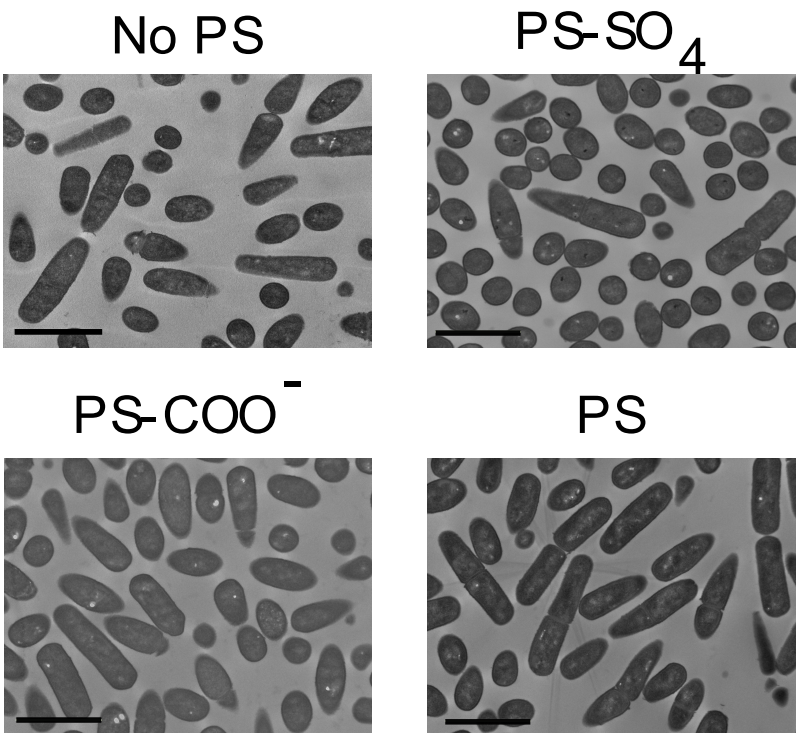

Figure S6. Negatively charged nanoplastics did not interact with *B. subtilis*. TEM images of bacteria without nanoplastics (No PS) and with negatively charged polystyrene nanoplastics (PS-SO_4, PS-COO-, non-functionalized PS). Scale bar is 2 μm.

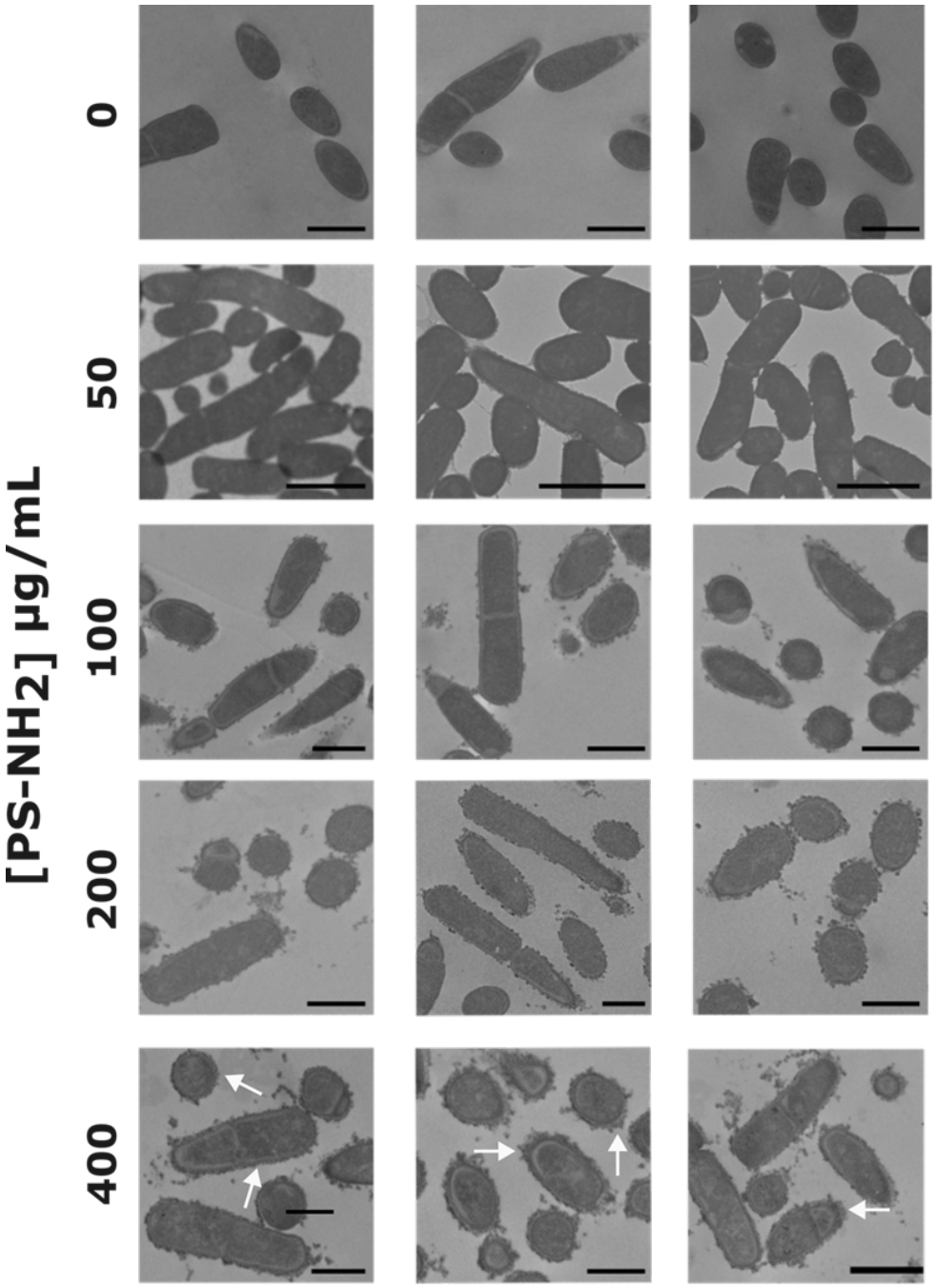

Figure S7. Concentration-dependent multilayer coating of PS-NH_2. Transmission electron microscopy (TEM) images of OD 0.2 *Bacillus subtilis* showing concentration-dependent multilayer surface coverage of positively charged PS-NH_2 immediately after 30-min treatment in water. White arrows point to multilayer nanoplastic coatings on certain regions of the bacterial surface. Scale bar: 1 µm.

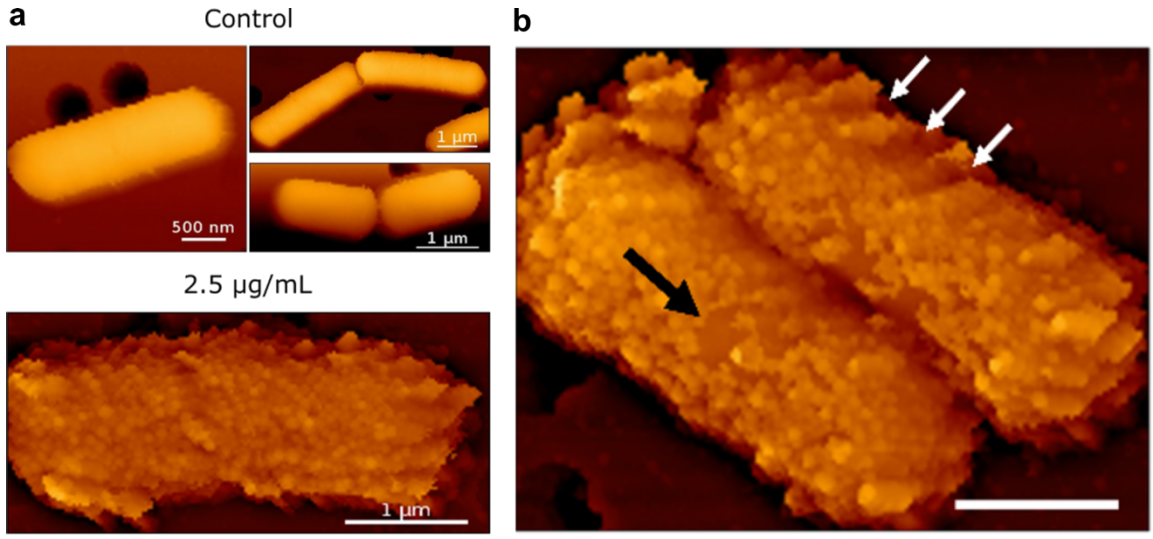

Figure S8. Additional AFM images of *B. subtilis* after 3 hours of growth in LB. (a) A bacterium showing nanoplastics "flaking-off" the surface (lower panel). (b) White arrows highlight a helical pattern along the cylindrical axis of *B. subtilis* that is free of nanoplastics, while the black arrow points to nanoplastic-free regions in the central part of the cell.

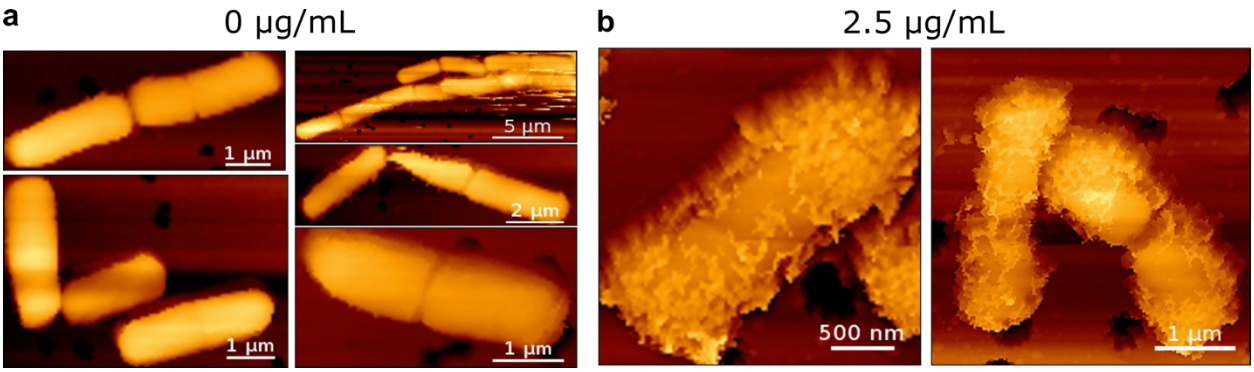

Figure S9. **Nanoplastic corona formation after 5 hours of growth in liquid medium.** (a) AFM images of *B. subtilis* without PS-NH_2 exposure and (b) pre-treated with 2.5 µg/mL PS-NH_2 (lower panel), showing nanoplastics being pushed away and forming a "nanoplastic corona" surrounding the bacterial surface.

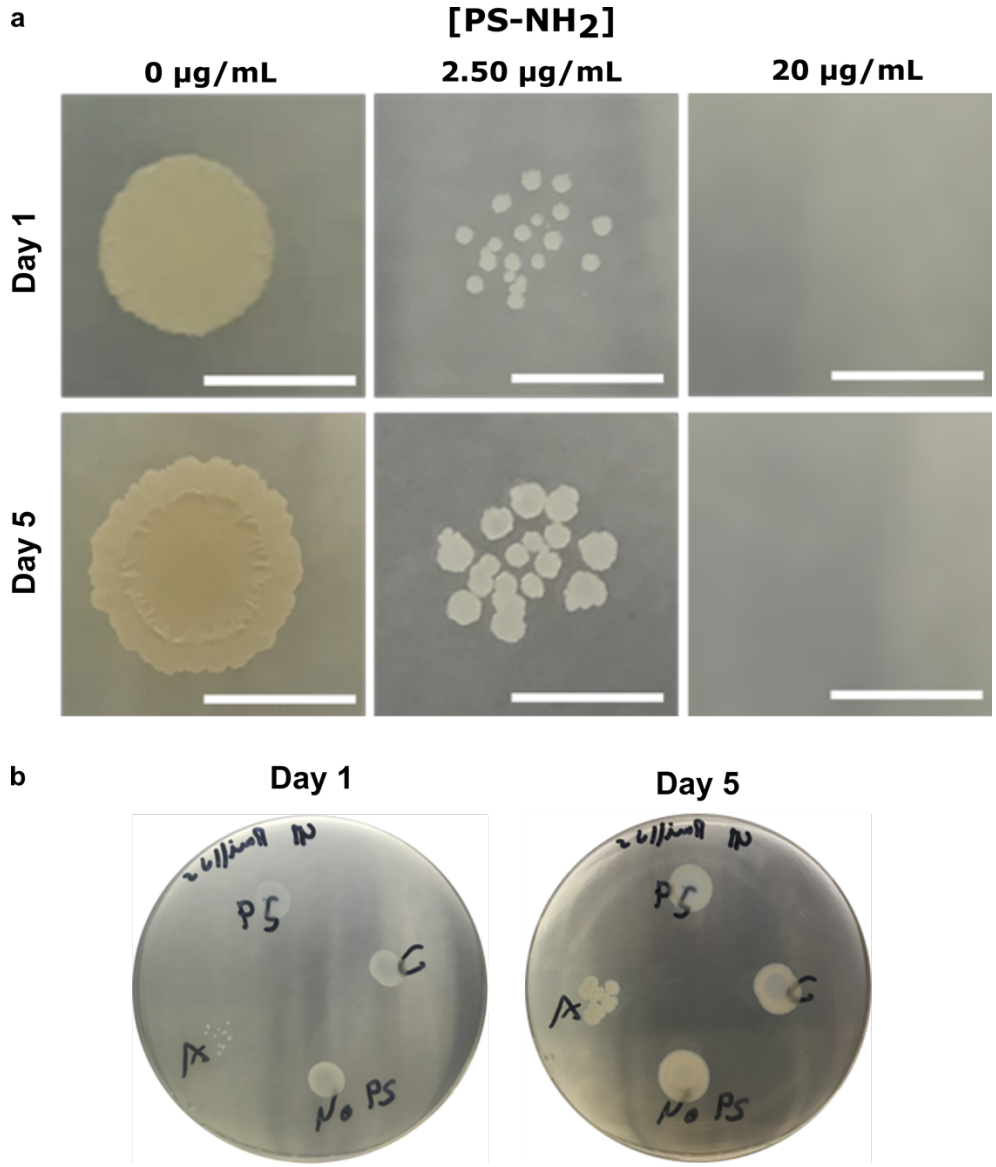

Figure S10. PS-NH_2 inhibits biofilm formation even on LBGM agar, while negatively charged nanoplastic do not prevent colony growth. (a) Representative images of biofilms grown on LBGM agar for 1-5 days following a 30-min exposure to PS-NH_2. (b) Representative images of biofilms grown on LB agar for 1-5 days following a 30-min exposure to 2.5 µg/mL negatively charged PS (100 nm) or PS-COO^- (30 nm). All images were taken from the top of the agar plate and are representative of three independent replicates across three trials. Similar results were observed for negatively charged nanoplastics at all tested concentrations. Scale: 1 cm.

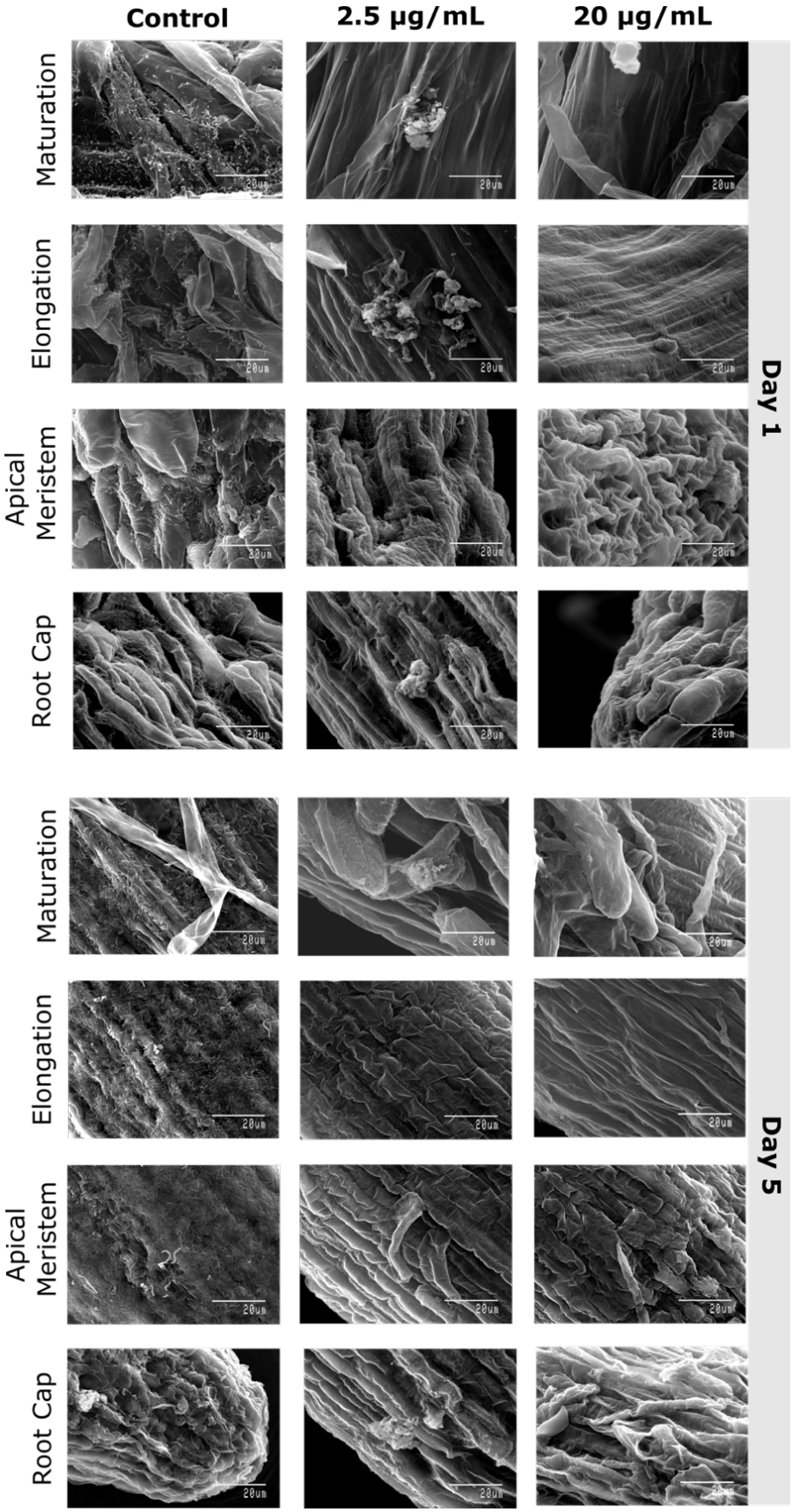

Figure S11. PS-NH_2 exposure impairs *B. subtilis* ability to colonize tomato roots. Scanning electron microscopy (SEM) images of *B. subtilis* on different regions (root cap, apical meristem, elongation, maturation) of the tomato root, one day (Day 1, top panel) and 5 days (Day 5, bottom panel) after exposure to 2.5 µg/mL (middle panel) and 20 µg/mL (rightmost panel) PS-NH_2. T control represents no exposure to nanoplastics (leftmost panel).